

Water-Soluble Pyrazolo[4,3-*e*][1,2,4]triazolo[1,5-*c*]pyrimidines as Human A₃ Adenosine Receptor Antagonists

Pier Giovanni Baraldi,^{*,†} Giulia Saponaro,[†] Romeo Romagnoli,[†] Mojgan Aghazadeh Tabrizi,[†] Stefania Baraldi,[†] Allan R. Moorman,^{§,#} Sandro Cosconati,^{||} Salvatore Di Maro,[⊥] Luciana Marinelli,[⊥] Stefania Gessi,[‡] Stefania Merighi,[‡] Katia Varani,[‡] Pier Andrea Borea,[‡] and Delia Preti[†]

[†]Dipartimento di Scienze Farmaceutiche and [‡]Dipartimento di Medicina Clinica e Sperimentale-Sezione di Farmacologia, Università di Ferrara, 44100 Ferrara, Italy

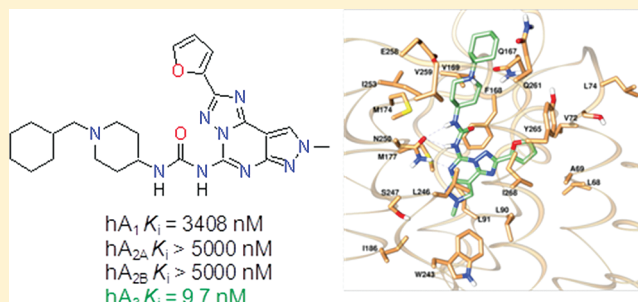
[§]King Pharmaceuticals, Inc., Research and Development, 4000 CentreGreen Way, Suite 300, Cary, North Carolina 27513, United States

^{||}Dipartimento di Scienze Ambientali, Seconda Università di Napoli, Via Vivaldi 43, 81100 Caserta, Italy

[⊥]Dipartimento di Chimica Farmaceutica e Tossicologica, Università "Federico II", Via D. Montesano 49, 80131 Napoli, Italy

Supporting Information

ABSTRACT: A relevant problem of the pyrazolo[4,3-*e*]-[1,2,4]triazolo[1,5-*c*]pyrimidine nucleus, an attractive scaffold for the preparation of adenosine receptor antagonists, is the low water solubility. We originally functionalized the C⁵ position with a salifiable 4-pyridylcarbamoyl moiety that conferred good water solubility at low pH (<4.0) but poor solubility at physiologic pH, indicative of the dissociation of the pyridinium species. Here we replaced the pyridin-4-yl moiety with a 1-(substituted)piperidin-4-yl ring to exploit the higher basicity of this nucleus and for the possibility to generate stable, water-soluble salts. The hydrochloride salt of the 1-(cyclohexylmethyl)piperidin-4-yl derivative (**10**, $K_i(\text{hA}_3) = 9.7 \text{ nM}$, $\text{IC}_{50}(\text{hA}_3) = 30 \text{ nM}$, $K_i(\text{hA}_1/\text{hA}_3) = 351$, $K_i(\text{hA}_{2A}/\text{hA}_3) > 515$, $\text{IC}_{50}(\text{hA}_{2B}) > 5 \mu\text{M}$) showed a solubility of 8 mg/mL at physiological pH and gave a stable aqueous system suitable for intravenous infusion. Molecular modeling studies were helpful in rationalizing the available structure–activity relationships and the selectivity profile of the new ligands.



INTRODUCTION

Adenosine, a ubiquitous nucleoside essential for the proper functioning of every cell in mammalian species is directly linked to energy metabolism through ATP, ADP, and AMP, while at the extracellular level it regulates a wide range of biological functions through activation of specific receptors (adenosine receptor, AR).^{1–4} These adenosine receptors belong to the superfamily of the G-protein-coupled receptors (GPCRs) and are classified as A₁, A_{2A}, A_{2B}, and A₃.

The A₃AR subtype is the most recently characterized member of the family.⁴ Activation of the subtype has been shown to inhibit adenylate cyclase, to increase phosphatidylinositol-specific phospholipase C and D activity, to elevate intracellular Ca²⁺ and IP₃ (inositol 1,4,5-trisphosphate) levels, and to enhance the release of inflammatory and allergic mediators from mast cells.^{5,6} The potential therapeutic applications derived from the modulation of this receptor subtype have been recently reviewed.^{7,8} It is becoming increasingly apparent that an antagonist of A₃AR might be therapeutically useful for the acute treatment of glaucoma.^{9,10} Specific antagonists are currently undergoing biological testing for their potential use in the treatment of stroke, neuro-

degenerative diseases, allergy, asthma, and COPD (Thomson Reuters Integrity source). Our group provided the first evidence that the A₃AR plays a role in colon tumorigenesis and, more importantly, can potentially be used as a diagnostic marker or a therapeutic target for colon cancer.¹¹

The pyrazolo[4,3-*e*][1,2,4]triazolo[1,5-*c*]pyrimidine (PTP) nucleus has been shown repeatedly to serve as an attractive scaffold for the preparation of adenosine receptor antagonists. Systematic substitution of the C²-, C⁵-, N⁷-, N⁸-, or C⁹-positions of PTPs^{7,12–16} allowed a structure–activity relationship (SAR) profile to be delineated for this class of molecules, primarily defining receptor subtype selectivity. A 2-furyl or a 2-(substituted)phenyl^{17,18} ring appeared important for affinity toward all four AR subtypes. The presence of a free amine at the C⁵-position combined with an arylalkyl moiety at the N⁷-position was found to significantly promote both affinity and selectivity at the A_{2A}AR subtype.¹² In contrast, introduction of an arylurea moiety at the C⁵-position and small alkyl chains (e.g., methyl or propyl) at the N⁸-position led to the

Received: March 6, 2012

Published: May 9, 2012

identification of highly potent and selective human A_3 AR antagonists.¹⁹ Notable in this class is the PTP analogue bearing a 4-(methoxy)phenylcarbamoyl moiety at C⁵ and an *n*-propyl group at N⁸ (MRE-3008-F20, **1**, Figure 1), which displayed a K_i of 0.29 nM at the human A_3 receptors expressed in CHO cells with high selectivity over hA_1 and hA_{2A} ARs (K_i of 1100 and 141 nM, respectively).²⁰

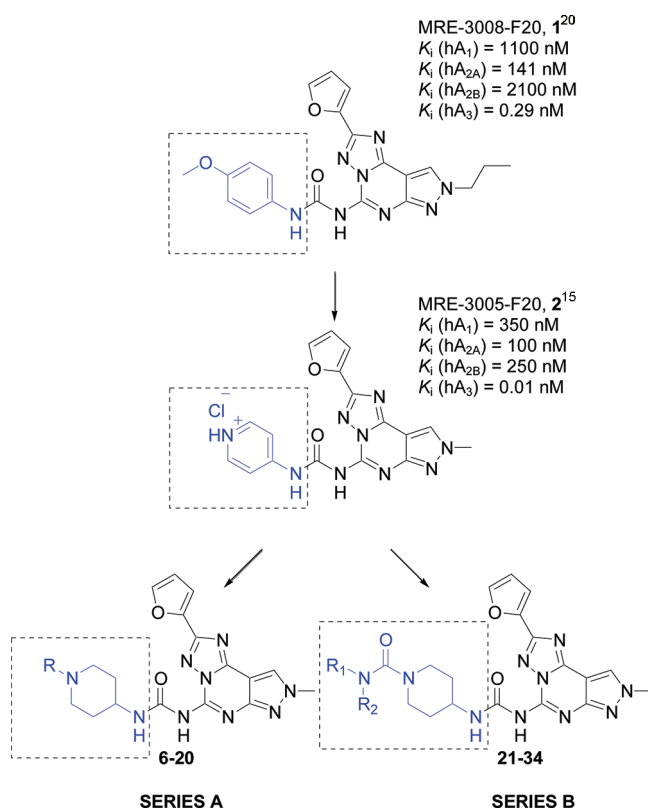


Figure 1. Pyrazolo[4,3-*e*][1,2,4]triazolo[1,5-*c*]pyrimidine: from pyridineurea to piperidineurea derivatives.

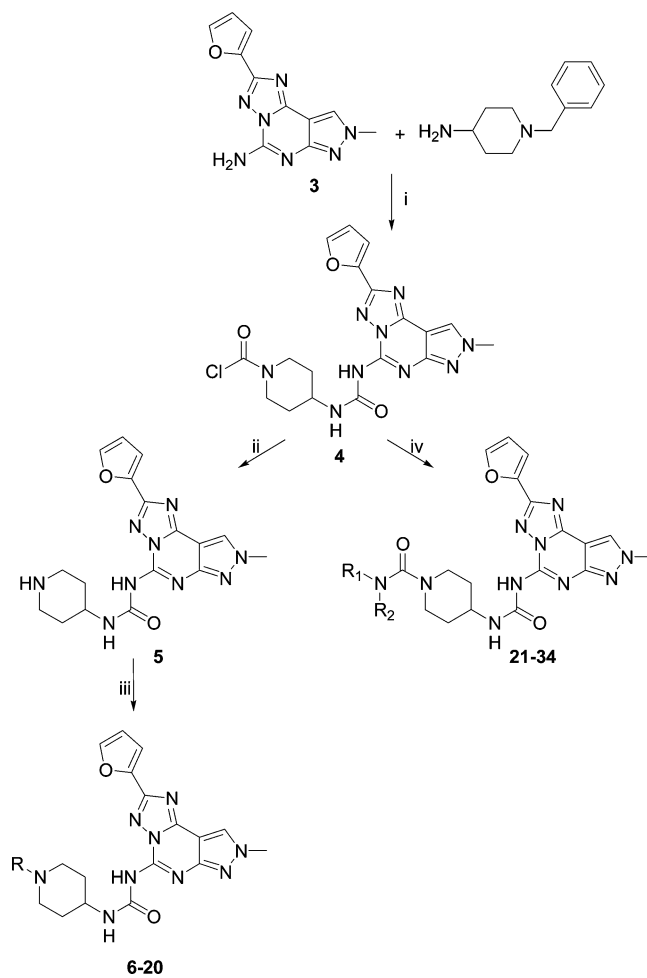
This class of molecules was found to synergistically enhance cytotoxic treatment of melanoma cells countering P-glycoprotein efflux in multidrug resistance.²¹ Nevertheless, a relevant problem of the PTPs was the typically low water solubility, which also limited their use as pharmacological and diagnostic tools. To enhance the water solubility, we originally replaced the phenylcarbamoyl moiety of **1** with a salifiable pyridin-4-ylcarbamoyl group. This led to the identification of the most potent hA_3 antagonist known to date (MRE-3005-F20, **2**, Figure 1).¹⁵ On the basis of our knowledge that the adenosine A_3 receptor was expressed at elevated levels in certain cancers,²¹ we wished to evaluate this class of adenosine A_3 antagonists for use in conjunction with various cytotoxic agents. We envisioned that these compounds would be administered by intravenous infusion. Although the aqueous solubility of **2** (approximately 11 mg/mL) was significantly enhanced, relative to that of **1**, aqueous formulations required a pH below 3.5 to obtain a homogeneous solution capable of being filter-sterilized. At a more physiologically acceptable pH (7.0–7.5), the solubility of **2** dropped to less than 0.1 mg/mL, affording a thick, unfilterable suspension (unpublished data). The present work is an extension of our SAR studies on **2**, in which we focused our attention on the pyridine ring. Specifically, we hypothesized that by converting the pyridin-4-yl-moiety to a 1-(substituted)-

piperidin-4-yl-ring, a suitable compound could be identified with significant potency at the target adenosine A_3 receptor, adequate selectivity toward other adenosine receptors, and appropriate aqueous solubility at physiologic pH due to the increased basicity of the ring nitrogen. For that reason we prepared a first series of *N*-[2-(2-furyl)-8-methyl-8*H*-pyrazolo[4,3-*e*][1,2,4]triazolo[1,5-*c*]pyrimidin-5-yl]-*N'*-(1-(substituted)-piperidin-4-yl)urea derivatives (series A, compounds **6–20**, Figure 1). Representative compounds were then converted into the corresponding hydrochloride salts, and the solubility at a physiologic pH of 7.4 (phosphate-buffered saline, PBS) was evaluated. The SAR study was then extended to a second series of *N*-substituted 4-[[[2-(2-furyl)-8-methyl-8*H*-pyrazolo[4,3-*e*][1,2,4]triazolo[1,5-*c*]pyrimidin-5-yl]amino]carbonyl]amino]-piperidine-1-carboxamide derivatives (series B, compounds **21–34**, Figure 1), with which we intended to probe the steric tolerance in the region around the piperidine nitrogen.

CHEMISTRY

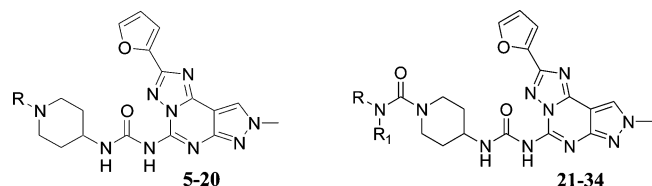
Scheme 1 depicts the preparation of final compounds **5–34** starting from 2-(2-furyl)-8-methyl-8*H*-pyrazolo[4,3-*e*][1,2,4]triazolo[1,5-*c*]pyrimidin-5-amine **3**, which was prepared as

Scheme 1^a



^aReagents and conditions: (i) (a) triphosgene, THF, CH_2Cl_2 , 0 °C, 15 min; (b) 140 °C, 50 min; (ii) TFA, CH_3CN/H_2O , 80 °C, 2 h; (iii) RX , K_2CO_3 , DMF, rt, 2–4 h; (iv) primary and secondary amines, TEA, 1,4-dioxane, 0 °C, 1 h, then rt, 3 h.

Table 1. Biological Data of the Synthesized Compounds



| compd | R | R ₁ | A ₁ K _i (nM) ^a | A _{2A} K _i (nM) ^b | A _{2B} IC ₅₀ (nM) ^c | A ₃ K _i (nM) ^d |
|-----------------|-----------------------------------|----------------|---|--|--|---|
| 5 | H | | >5000 | >5000 | 2428 (2037–2894) | 65 (56–75) |
| 6 | Me | | >5000 | >5000 | >5000 | 253 (211–303) |
| 7 | propyl | | 2794 (2351–3322) | 1193 (992–1434) | >5000 | 71 (51–98) |
| 8 | allyl | | 3357 (3045–3701) | 1423 (1117–1811) | >5000 | 51 (39–67) |
| 9 | propargyl | | 802 (707–910) | 789 (725–859) | >5000 | 25 (22–29) |
| 10 | cyclohexyl-CH ₂ | | 3408 (3043–3817) | >5000 | >5000 | 9.7 (7.6–12.4) |
| 11 | Bn | | 703 (641–770) | 526 (473–585) | 2061 (1589–2672) | 30 (25–38) |
| 12 | 4-F-Bn | | 1049 (868–1269) | >5000 | >5000 | 24 (19–31) |
| 13 | 4-Cl-Bn | | 724 (626–838) | >5000 | >5000 | 26 (20–32) |
| 14 | 4-CH ₃ -Bn | | 1478 (1254–1740) | >5000 | >5000 | 13.8 (9.2–20.6) |
| 15 | 4-OCH ₃ -Bn | | 1156 (1028–1299) | >5000 | >5000 | 13.3 (11.9–14.9) |
| 16 | 4-CN-Bn | | 166 (124–224) | 2223 (2016–2452) | >5000 | 11.8 (8.2–17.0) |
| 17 | 4-NO ₂ -Bn | | 371 (290–474) | >5000 | >5000 | 12.4 (9.7–16.0) |
| 18 | 3-pyridin-CH ₂ | | 1329 (1071–1649) | >5000 | >5000 | 44 (37–52) |
| 19 | 4-pyridin-CH ₂ | | 1188 (949–1488) | >5000 | >5000 | 39 (33–46) |
| 20 | EtO ₂ CCH ₂ | | 348 (267–453) | 1084 (915–1283) | >5000 | 12.2 (8.4–17.7) |
| 21 | Et | H | 1500 (1320–1690) | >5000 | >5000 | 30 (22–41) |
| 22 | isopropyl | H | 1324 (1164–1508) | >5000 | >5000 | 9.8 (7.9–12.2) |
| 23 | cyclopentyl | H | 744 (598–927) | >5000 | >5000 | 9.3 (6.2–13.9) |
| 24 | cyclohexyl | H | 761 (611–949) | >5000 | >5000 | 13.7 (9.8–19.1) |
| 25 | cycloheptyl | H | 805 (665–973) | >5000 | >5000 | 7.7 (5.5–10.8) |
| 26 | Bn | H | 525 (441–625) | >5000 | 1107 (934–1311) | 8.1 (6.0–10.9) |
| 27 | 2-phenylethyl | H | 182 (128–259) | 1842 (1695–2001) | 1755 (1567–1967) | 6.8 (4.8–9.5) |
| 28 | 3-phenylpropyl | H | 112 (80–158) | 1641 (1467–1835) | 1542 (1405–1695) | 14.5 (11.4–18.5) |
| 29 | 4-F-Bn | H | 408 (335–499) | 3255 (3098–3420) | 1042 (897–1210) | 4.9 (2.9–8.1) |
| 30 | 4-Cl-Bn | H | 614 (490–768) | 1137 (1034–1249) | 505 (398–638) | 25 (16–39) |
| 31 | 4-CH ₃ -Bn | H | 396 (335–442) | 2813 (2584–3061) | 2122 (1929–2335) | 3.9 (2.2–6.9) |
| 32 | 4-OCH ₃ -Bn | H | 635 (524–771) | >5000 | 3244 (3028–3476) | 10.4 (6.2–17.4) |
| 33 ^e | 4-pyridyl | H | 1299 (936–1803) | 1856 (1498–2300) | 3235 (2744–3813) | 21 (14–30) |
| 34 ^e | 4-methylpiperazinyl | | 1123 (929–1356) | 1282 (1050–1565) | 2144 (1674–2745) | 31 (26–38) |

^aDisplacement of specific [³H]DPCPX binding to human A₁ARs expressed in CHO cells (K_i, nM). ^bDisplacement of specific [³H]ZM241385 binding to human A_{2A}ARs expressed in CHO cells (K_i, nM). ^ccAMP assay in CHO cells expressing hA_{2B}ARs (IC₅₀, nM). ^dDisplacement of specific [³H]MRE-3008-F20 binding to human A₃ARs expressed in CHO cells (K_i, nM). Data are expressed as geometric mean with 95% confidence limits in parentheses of three or four independent experiments performed in duplicate. ^eTrifluoroacetate salt.

previously described by us.²² In the first step, the commercially available 1-benzyl-4-aminopiperidine was treated with triphosgene at 0 °C for 15 min, leading to the formation of the corresponding 4-isocyanatopiperidine derivative as established by IR spectroscopy. This was then reacted with the tricyclic amine (**3**) at 140 °C for 50 min. Under these conditions we observed the formation of the carbamoyl chloride derivative (**4**) as a result of the concurrent cleavage of the *N*-benzyl moiety and conversion into the corresponding carbamoyl chloride function. This confirmed the known capability of triphosgene to cleave *N*-benzyl-protected secondary amines.^{23,24}

The carbamoyl chloride derivative **4** was then hydrolyzed in the presence of TFA and a mixture of CH₃CN/H₂O as solvent to give the unsubstituted piperidine derivative (**5**), which was subjected to *N*-alkylation under standard conditions with alkyl/cycloalkyl/(hetero)arylalkyl halides to afford the final compounds **6–20**. The bis-urea derivatives **21–34** were obtained in good yields via the treatment of the carbamoyl chloride **4** with the appropriate primary or secondary amines.

RESULTS AND DISCUSSION

All of the synthesized compounds (**5–34**) were evaluated in radioligand binding assays to determine their affinities for human A₁, A_{2A}, and A₃ adenosine receptors using [³H]DPCPX (1,3-[³H]dipropyl-8-cyclopentylxanthine), [³H]ZM241385 (4-(2-[7-amino-2-(2-furyl)[1,2,4]triazolo[2,3-*a*][1,3,5]triazin-5-ylamino)ethyl)phenol), [³H]MRE-3008-F20 (5-*N*-(4-methoxyphenylcarbamoyl)amino-8-propyl-2-(2-furyl)pyrazolo[4,3-*e*]-1,2,4-triazolo[1,5-*c*]pyrimidine), respectively, as radioligands. Efficacy of the compounds versus hA_{2B}AR was investigated by evaluating their capability to inhibit NECA (5'-(*N*-ethylcarboxamido)adenosine)-stimulated (100 nM) cAMP production. Antagonism of selected ligands versus hA₃AR was also assessed through cAMP experiments evaluating their capability to block the inhibitory effect mediated by Cl-IB-MECA (2-chloro-*N*⁶-(3-iodobenzyl)adenosine-5'-*N*-methylcarboxamide). Affinity data for A₁, A_{2A}, and A₃ receptors (expressed as K_i values) and IC₅₀ values for hA_{2B} and hA₃

subtypes, derived from the cAMP assays, are listed in Tables 1 and 2, respectively.

Table 2. Potency of Selected Novel A₃AR Antagonists in hA₃CHO Cells on cAMP Production^a

| compd | A ₃ IC ₅₀ (nM) | compd | A ₃ IC ₅₀ (nM) |
|-------|--------------------------------------|-------|--------------------------------------|
| 5 | 262 (203–338) | 20 | 41 (35–47) |
| 6 | 910 (846–978) | 21 | 116 (91–148) |
| 7 | 301 (271–335) | 22 | 34 (24–47) |
| 8 | 212 (171–263) | 23 | 30 (24–39) |
| 9 | 105 (83–131) | 24 | 44 (33–59) |
| 10 | 30 (22–41) | 25 | 26 (17–38) |
| 11 | 121 (100–146) | 26 | 29 (18–46) |
| 12 | 82 (66–101) | 27 | 23 (14–37) |
| 13 | 91 (80–104) | 28 | 46 (30–72) |
| 14 | 50 (43–58) | 29 | 15 (10–25) |
| 15 | 45 (37–56) | 30 | 90 (81–99) |
| 16 | 40 (33–48) | 31 | 12 (8–19) |
| 17 | 42 (33–54) | 32 | 34 (28–41) |
| 18 | 180 (162–199) | 33 | 82 (71–96) |
| 19 | 166 (140–197) | 34 | 120 (103–140) |

^aData are expressed as geometric mean with 95% confidence limits in parentheses of three or four independent experiments performed in duplicate.

Structure–Activity Relationship Analysis: hA₃AR Affinity. All of the synthesized molecules exhibited good affinities at the hA₃AR subtype with K_i values ranging from 3.9 (compound 31, Table 1) to 253 nM (compound 6). Nevertheless, compound 5, bearing an unsubstituted piperidine ring at the C⁵-position, showed a remarkable (6500-fold) decrease of hA₃AR affinity compared to its unsaturated congener 2. Considering that piperidine and pyridine have a comparable steric bulk (with a calculated van der Waals surface area of 175.57 and 128.26 Å³, respectively),²⁵ the higher basicity (pK_b of 2.7 for piperidine vs 8.7 for pyridine) and lower lipophilicity (cLogD calculated at pH 7.4 of –2.15 for piperidine and 0.75 for pyridine) of piperidine could be responsible for this marked decrease in affinity. With the perspective of exploiting the higher basicity of piperidine and its possibility to generate stable and water-soluble salts, we tried to enhance the affinity/selectivity of compound 5 by substitution of the piperidine nitrogen.

The initial strategy was alkylation of the N¹-position of the piperidine ring to obtain the compounds of series A (Figure 1). Among the N¹-(1-alkyl/arylalkylpiperidin-4-yl)urea derivatives 6–20, the introduction of a methyl group at the piperidine nitrogen, as in compound 6, led to a 4-fold decrease of A₃AR affinity compared to the corresponding N-unsubstituted derivative 5. Introduction of a propyl moiety resulted in a substantial maintenance of A₃ affinity (see compound 7 vs 5). The effect of unsaturated chains was evaluated with the N-allyl derivative 8 and N-propargyl derivative 9. The latter compound showed a 2.5-fold increase of affinity when compared with 5, while the N-allyl substitution was almost equipotent. A more marked effect on binding properties was observed when a bulky cycloalkylmethyl substituent was introduced. The affinity of the N-cyclohexylmethyl derivative 10 was almost 7-fold greater than that of the N-unsubstituted derivative 5. Although unsaturation in straight-chain aliphatic substituents led to improved affinity (see compound 7 vs 8 vs 9), this pattern was

not seen by replacing the N-cyclohexylmethyl derivative (10) with the N-benzyl derivative (11).

While the N-benzyl derivative (11) had lower affinity than the corresponding N-cyclohexylmethyl derivative, this substitution led to a slight improvement of affinity over the unsubstituted derivative (see compound 11 vs 5). This effect was enhanced occasionally by *p*-substitution of the benzyl group (derivatives 12–17). In this regard, both electron withdrawing and electron donating functions have been examined, but we did not observe a clear correlation between binding affinity and the electronic properties of the introduced moieties, as both strong electron-withdrawing (i.e., compound 16, 17) or donating (compound 15) functions seem to promote comparable outcomes in terms of A₃AR affinity.

Compounds 18 and 19, in which a heteroarylalkyl moiety has been introduced at the piperidine nitrogen, display similar binding potencies as the corresponding arylalkyl bioisoster 11. A slight increase of A₃AR affinity was observed with compound 20, deriving from the alkylation of 5 (see Scheme 1) with 2-bromoethylacetate.

The bis-urea derivatives 21–34 (series B, Figure 1) afforded A₃ affinities in the low nanomolar range. Among the N-alkyl-substituted derivatives 21–25, a slight preference for bulky and lipophilic cycloalkyl substitution can be noted. For example, the N-cycloheptyl derivative (25) displayed an almost 4-fold increase of affinity when compared to the N-ethyl derivative 21. Nevertheless, in light of the affinity data for the N-(substituted)arylalkyl derivatives 26–31 (K_i values ranging from 3.9 to 25 nM), it appeared that A₃ binding potency seems poorly related to structural modifications of the terminal portion of the chain at the C⁵-position of the pyrazolotriazolopyrimidine nucleus. The maintenance of affinity in the same range of concentration for N-4-pyridyl and 4-methylpiperazinyl derivatives, 33 and 34, respectively, support such an observation.

Where possible, pairwise comparison between the K_i (hA₃) values of compounds of series A and series B resulted in a substantial maintenance or a slight increase of affinity in most cases for the bis-urea derivatives (i.e., compounds 11–15 vs 26, 29–32, respectively). Among these, the 4-CH₃-benzyl substituted 31 is identified as the most potent hA₃AR ligand reported herein, with a K_i of 3.9 nM.

Structure–Activity Relationship Analysis: hA₃AR vs hA_{2A}AR and hA₁AR Selectivity. All of the examined molecules exhibited a clear selectivity toward the hA₃AR versus both hA₁ and hA_{2A} AR subtypes. The K_i values at the A_{2A} subtype were, in most cases, higher than 1 μM (except for compounds 9 and 11, which displayed high nanomolar affinity for the target). The hA₁/hA₃ selectivity ratios appeared highly variable within the two series. While different substitutions at the piperidine nitrogen did not seem to remarkably affect hA₃ affinity, the hA₁AR subtype appeared, indeed, quite responsive to steric/electronic modulation of this part of the molecule.

Among compounds of series A, the affinity for the hA₁AR appeared particularly relevant when the piperidine nitrogen was substituted with benzyl moieties bearing strong electron withdrawing groups in the *p*-position. The 4-CN (16) and the 4-NO₂ (17) derivatives exhibited the highest hA₁ affinities (K_i (hA₁) values of 166 and 371 nM, respectively), and compound 16 stands out as the least selective A₃ ligand of this subset of molecules (K_i (hA₁/hA₃) = 14). Interestingly, *p*-substitution with electron donating groups reduced hA₁ affinities, improving hA₃AR vs hA₁ selectivity (see compounds

14 and **15** with $K_i(\text{hA}_1/\text{hA}_3)$ ratios of 107 and 87, respectively). *N*-(Cyclo)alkyl substitution seemed to be less well tolerated than *N*-arylalkyl substitution by the hA_1 subtype, promoting hA_3 vs hA_1 selectivity. The *N*-cyclohexylmethyl derivative (**10**) was the most selective compound of the entire series ($K_i(\text{hA}_1/\text{hA}_3) = 351$).

To varying degrees, the *N*-arylalkyl derivatives of series B were found to be preferred over the corresponding *N*-(cyclo)alkyl derivatives for enhancing hA_1 AR affinity. It was observed that hA_1 AR affinity seemed to be related to the distance between the aromatic nucleus and the ureidic nitrogen. In particular, the comparison of the binding profiles for the 3-phenylpropyl-substituted **28** ($K_i(\text{hA}_1) = 112$ nM) and the inferior homologues 2-phenylethyl **27** ($K_i(\text{hA}_1) = 182$ nM) and benzyl **26** ($K_i(\text{hA}_1) = 525$ nM) reveals that binding affinity proportionately increases with the elongation of the alkyl spacer, which makes compound **28** the least selective A_3 ligand of both of the analyzed series ($K_i(\text{hA}_1/\text{hA}_3) = 7.7$).

Because of the lack of an adequate number of closely related analogues, it is difficult to identify clear differences in the selectivity profiles between the two series. However, a comparison between the binding pattern of compounds **11**–**15** (series A) and the analogously substituted **26**, **29**–**32** (series B) would suggest that the additional urea moiety of series B is slightly preferred for promoting A_3 versus A_1 selectivity.

Functional Assays: hA_{2B} and hA_3 ARs. As reported in Table 1, the examined compounds showed very low or no activity at the hA_{2B} AR subtype, with $\text{IC}_{50} > 1$ μM (except for compound **30** with $\text{IC}_{50} = 505$ nM). For 20 out of 31 compounds tested, $\text{IC}_{50} > 5$ μM was found.

The compounds of both series were shown to behave as antagonists of the hA_3 AR subtype in the cAMP functional assay (Figure 2B and Table 2). A good correspondence between binding and functional experiments was observed. The molecules showing the best affinities for hA_3 AR also displayed very high potency in receptor inhibition (IC_{50} values in the low nanomolar range). Derivative **31**, showing the highest hA_3 affinity ($K_i = 3.9$ nM), emerged as the most potent compound of the series, with an IC_{50} of 12 nM.

Molecular Modeling Studies. To rationalize the SAR data presented, docking simulations were performed using the hA_3 AR model previously published by our research group.²⁶ In this work the recently published crystal structure of the hA_{2A} receptor (PDB code 3EML)²⁷ in complex with compound ZM241385 was used to obtain a homology model of the hA_3 ARs. The sequence alignment between the three receptors and the positions of the disulfide bridges were attained consistently with what was already suggested by Moro and co-workers.²⁸ The structure of the modeled receptor was used with Glide to perform docking calculations of compound **10**, which displayed good affinity for the hA_3 receptor (9.7 nM) and the best selectivity profile ($K_i(\text{hA}_1/\text{hA}_3) = 351$, $K_i(\text{hA}_{2A}/\text{hA}_3) > 515$) among compounds from both series. The docking poses obtained were evaluated for their consistency with the available SAR data, as well as for the Glide scores obtained from these calculations. Results obtained for **10** revealed that for the best Glide score (-7.435), the ligand binds to the outer portion of the A_3 AR being surrounded by TM helices 3, 5, 6, and 7 and EL2. This predicted binding pose strongly resembles one calculated for some analogues reported by other authors.¹⁸ In this position, the core ligand scaffold establishes a π -stacking interaction with F168 and two H-bonds with the N250 side chain, which was demonstrated to be critical for ligand binding

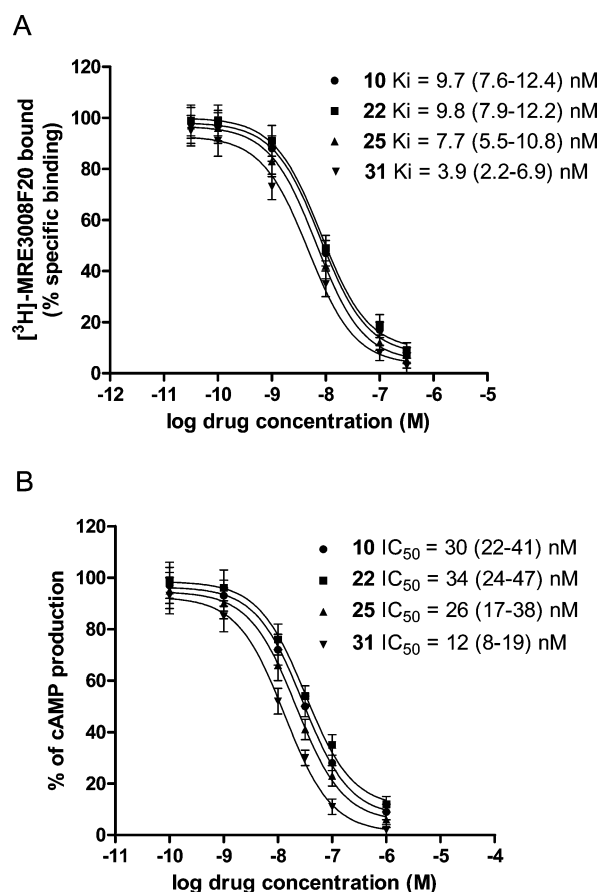


Figure 2. Competition binding and cAMP assays of selected novel A_3 AR compounds: affinity and potency values expressed as K_i (A) and IC_{50} (B), respectively.

in the hA_3 AR, as well as being highly conserved in all of the ARs (Figure 3).²⁹

In this position the methyl group at N⁸ points downward toward the inner part of the receptor, making contacts with W243 and being surrounded by hydrophobic residues (L91, M177, I186, L246, and S247). It is noteworthy that the interaction with W243 should be considered to be responsible for the antagonist properties of this ligand, as already demonstrated for other AR antagonists.¹⁸ Hydrophobic contacts are also established by the furyl ring with the receptor pocket formed by TM helices 2, 3, and 7, made up by L68, A69, V72, Y265, and I268. However, in this theoretical binding pose, the R substituent of **10** points toward the external part of the receptor at the crevice of TMS and TM6 where the terminal cyclohexyl ring makes contact with Q261 and Q167. Interestingly, as observed with other hA_3 AR antagonists,²⁶ the favorable interaction with the outer portion of TMS, TM6, EL2, and EL3 seems to be the reason for the observed selectivity of these compounds. In particular, in the hA_1 , hA_{2A} , and hA_{2B} ARs, salt bridges are established at the interface of EL2 and EL3, thus making this area narrower and less prone to be occupied by the ligand substituents (Figure 4a). On the other hand in the hA_3 AR this region appears to be wider to host the R substituent. Interestingly, the influence on A_3 AR ligand selectivity of the receptor area at the crevice between EL2 and EL3 was already postulated by us²⁶ and other authors²⁸ for different selective antagonists. Indeed, the ligand piperidine ring, while providing further interaction points with the

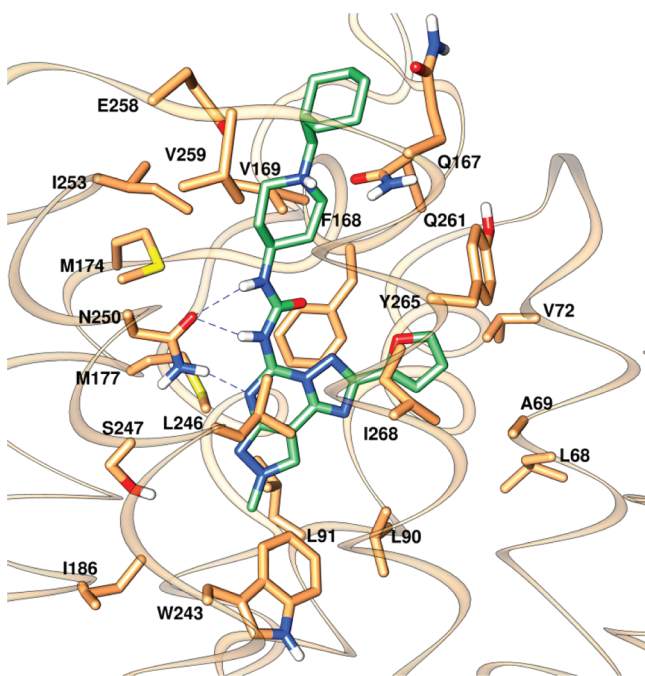


Figure 3. Close view of the calculated binding pose for **10** in the hA₃AR model. The ligand and receptor are depicted as green and sticks, respectively. H-Bonds are depicted as dashed blue lines.

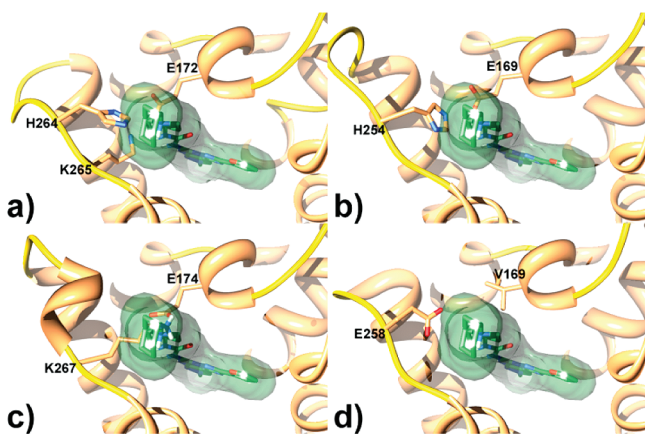


Figure 4. Superimposition of the structures of the A₁ (a),²⁶ A_{2A} (b),²⁷ A_{2B} (c),⁴² and hA₃ (d) ARs. Receptors are represented as ribbons and orange sticks. **10** is represented as green surface and sticks.

receptor, projects its nitrogen atom toward the external receptor region. This should explain why it can be N-alkylated with different substituents without significantly affecting the A₃AR affinity.

Water Solubility and Druglikeness Prediction. A few representative compounds were converted into the corresponding hydrochloride salts, and the water solubility at a physiological pH (7.4, PBS) was evaluated. While under these conditions the solubility of **2** dropped to less than 0.1 mg/mL; the piperidine derivatives **9**, **10**, and **12** were found to have a solubility of 8–10 mg/mL and gave stable aqueous systems suitable for evaluation as an intravenous infusion. As expected, the less lipophilic *N*-methyl derivative **6** was shown to be even more soluble (15 mg/mL). Nevertheless, considering the better binding profile, we selected compound **10** as a reference compound for molecular modeling studies (see above) and computational calculation of several druglikeness parameters

(see Table S1 of the Supporting Information). Most of the evaluated parameters were shown to be within the range of values representative of 95% of known drugs. Moreover, in view of the known metabolic lability of the 2-furan ring of PTPs¹⁸ we performed preliminary ligand-based calculations based on the SMARTCyp³⁰ approach to predict the sites of cytochrome P450 mediated metabolism on compound **10**. For each ligand atom this software calculated the propensity to be the site of metabolism (SOM). Figure 5 depicts compound **10** in which all

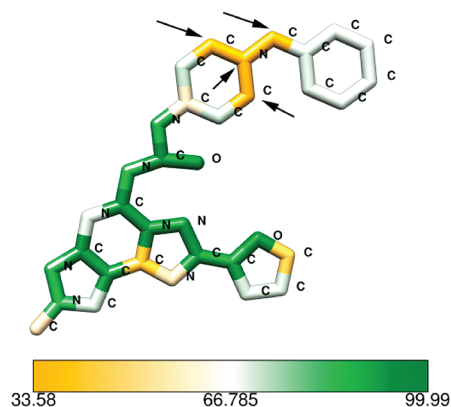


Figure 5. 2D representation of compound **10**. Atoms are colored according to the calculated SMARTCyp score (color coding is also reported). Arrows indicate the predicted SOMs for **10**.

heavy atoms were colored according to the relative SMARTCyp score. Interestingly, the software calculated for the piperidine nitrogen and the adjacent carbon atoms the highest propensity to be SOMs (lowest scores). As mentioned in the molecular modeling section, this region of the ligand should point toward the outer part of the receptor, so it can be postulated that the metabolites of **10** can also positively interact with the A₃AR. Also, one carbon atom of the furyl substituent appeared to be a putative SOM; nevertheless, from these calculations this atom does not appear to be as prone to react with cytochrome P450.

CONCLUSION

In the present work we synthesized two series of compounds in which the 4-pyridinyl moiety of our reference hA₃AR antagonist **2**¹⁵ (Figure 1) was replaced by a 1-(substituted)-piperidin-4-yl ring. Derivatives of series A (Table 1), in which the piperidine nitrogen was alkylated with different (cyclo)-alkyl/arylalkyl moieties, were designed with the perspective of exploiting the higher basicity of piperidine and its possibility to form stable, water-soluble salts. This approach was evaluated in order to overcome solubility problems encountered with the pyridine derivative **2** while trying to prepare aqueous formulations at a physiological pH suitable for intravenous infusion.

All of the synthesized molecules exhibited good affinity and selectivity at the hA₃AR subtype, with *K_i* in the low nanomolar range. The 1-(cyclohexylmethyl)piperidin-4-yl derivative **10** showed the best binding profile in terms of hA₃ affinity (*K_i* = 9.7 nM), potency (IC₅₀ = 30 nM), and selectivity (*K_i*(hA₁/hA₃) = 351, *K_i*(hA_{2A}/hA₃) > 515, IC₅₀(hA_{2B}) > 5 μM). Molecular modeling studies were helpful in rationalizing the observed structure–activity relationships, along with the selectivity profiles of the new series of ligands. Docking of compound

10 in complex with hA₃AR furnished a general model of the hypothetical binding mode for the newly described derivatives. Moreover, this compound, as the hydrochloride salt, proved to have a solubility of 8 mg/mL at physiological pH and gave a stable aqueous system suitable for intravenous infusion.

EXPERIMENTAL SECTION

Chemistry. Materials and Methods. Reaction progress and product mixtures were monitored by thin-layer chromatography (TLC) on silica gel (precoated F₂₅₄ Macherey-Nagel plates) and visualized by UV lamp (254 nm light source) or with aqueous potassium permanganate. Chromatography was performed on Merck 230–400 mesh silica gel. After extraction from aqueous phases, the organic solutions were dried over anhydrous sodium sulfate. Light petroleum refers to the fractions boiling at 40–60 °C. ¹H NMR data were determined in CDCl₃ or DMSO-*d*₆ solutions with a Varian VXR 200 spectrometer or a Varian Mercury Plus 400 spectrometer. Peak positions are given in parts per million (δ) downfield from tetramethylsilane as internal standard, and *J* values are given in hertz. Splitting patterns are designated as follows: s, singlet; d, doublet; t, triplet; q, quartet; m, multiplet; b, broad. All of the detected signals were in accordance with the proposed structures. Melting points for purified products were determined in a glass capillary on a Stuart Scientific electrothermal apparatus SMP3 and are uncorrected. Electrospray ionization mass spectrometry (ESI/MS) was performed with an Agilent 1100 series LC/MSD in positive scan mode using direct injection of the purified compound solution (MH⁺). Elemental analyses were performed by the microanalytical laboratory of Dipartimento di Chimica, University of Ferrara, Italy, and were within ±0.4% of the theoretical values for C, H, and N. All final compounds revealed a purity of not less than 95%.

Preparation of 4-[[[2-(2-Furyl)-8-methyl-8H-pyrazolo[4,3-*e*]-[1,2,4]triazolo[1,5-*c*]pyrimidin-5-yl]amino]carbonyl]amino]piperidine-1-carbonyl Chloride (4). A solution of 4-amino-1-benzylpiperidine (1.14 g, 6 mmol) in anhydrous THF (40 mL) was added in one portion to a solution of triphosgene (3 g, 10 mmol) in anhydrous CH₂Cl₂ (13 mL), previously cooled to 0 °C. TEA (triethylamine, 5 g, 50 mmol) was then added dropwise, and the resulting mixture was stirred at the room temperature for 15 min. The precipitate was filtered off and washed with THF. The filtrate was concentrated to give a brown oil. IR spectroscopy of the crude material confirmed the formation of the isocyanate species. 2-(2-Furyl)-8-methyl-8H-pyrazolo[4,3-*e*]-[1,2,4]triazolo[1,5-*c*]pyrimidin-5-amine 3 (0.5 g, 2 mmol) was added to the crude isocyanate, and the mixture was heated at 140 °C for 50 min without solvents. The mixture was slowly cooled to 0 °C, followed by the addition of methanol. The compound that precipitated was collected by filtration and repeatedly washed with methanol: white solid; 75% yield; mp 247 °C; ¹H NMR (DMSO-*d*₆) δ 9.25 (bd, *J* = 10.8 Hz, 1H), 8.77–8.71 (m, 2H), 7.98 (m, 1H), 7.29 (m, 1H), 6.77–6.74 (m, 1H), 4.12 (s, 3H), 3.98 (m, 1H), 3.35 (m, 2H), 3.16 (m, 2H), 2.08 (m, 2H), 1.61 (m, 2H). Anal. (C₁₈H₁₈ClN₉O₃) C, H, N. MS (ESI): [MH]⁺ = 444.85 (0%); 382.0 (100%).

Preparation of *N*-[2-(2-Furyl)-8-methyl-8H-pyrazolo[4,3-*e*]-[1,2,4]triazolo[1,5-*c*]pyrimidin-5-yl]-*N'*-piperidin-4-ylurea (5). Trifluoroacetic acid (200 μL) was added to a solution of 4 (0.5 g, 1.1 mmol) in a mixture of H₂O/CH₃CN (1:1, 60 mL), and the mixture was stirred at 80 °C for 2 h. The solvents were removed under reduced pressure, and the product was purified by crystallization from dichloromethane/diethyl ether: white solid; 91% yield; mp 208 °C; ¹H NMR (DMSO-*d*₆) δ 9.25 (bs, 1H), 8.86 (bm, 1H), 8.77–8.73 (m, 2H), 7.98 (m, 1H), 7.29 (m, 1H), 6.77–6.74 (m, 1H), 4.12 (m, 3H), 3.98 (m, 1H), 3.27 (m, 2H), 3.08 (m, 2H), 2.09 (m, 2H), 1.82 (m, 2H). MS (ESI): [MH]⁺ = 382.0. Anal. (C₁₇H₁₉N₉O₂) C, H, N.

General Procedure for the Preparation of *N*-[2-(2-Furyl)-8-methyl-8H-pyrazolo[4,3-*e*]-[1,2,4]triazolo[1,5-*c*]pyrimidin-5-yl]-*N'*-(1-substituted-piperidin-4-yl)urea Derivatives 6–20. To a solution of 5 (115 mg, 0.3 mmol) in DMF (10 mL) were added K₂CO₃ (45 mg, 0.33 mmol) and the appropriate alkyl halide (0.33

mmol). The mixture was stirred at room temperature for 2 h. The solvent was removed under reduced pressure, and the product was purified by column chromatography, eluting with EtOAc (ethyl acetate)/MeOH (9:1).

***N*-[2-(2-Furyl)-8-methyl-8H-pyrazolo[4,3-*e*]-[1,2,4]triazolo[1,5-*c*]pyrimidin-5-yl]-*N'*-(1-methylpiperidin-4-yl)urea (6).** White solid; 27% yield; mp 228 °C (dec); ¹H NMR (DMSO-*d*₆) δ 9.19 (bs, 1H), 8.77 (s, 1H), 8.73 (bd, *J* = 7.6 Hz, 1H), 7.99–7.97 (m, 1H), 7.30–7.28 (m, 1H), 6.77–6.74 (m, 1H), 4.12 (s, 3H), 3.89 (m, 1H), 3.39 (s, 3H), 3.08–2.90 (m, 2H), 2.44 (m, 2H), 1.99 (m, 2H), 1.89–1.56 (m, 2H). MS (ESI): [MH]⁺ = 396.3. Anal. (C₁₈H₂₁N₉O₂) C, H, N.

***N*-[2-(2-Furyl)-8-methyl-8H-pyrazolo[4,3-*e*]-[1,2,4]triazolo[1,5-*c*]pyrimidin-5-yl]-*N'*-(1-propylpiperidin-4-yl)urea (7).** White solid; 31% yield; mp 171 °C (dec); ¹H NMR (DMSO-*d*₆) δ 9.11 (bs, 1H), 8.81 (bd, *J* = 7.6 Hz, 1H), 8.69 (s, 1H), 7.96–7.95 (m, 1H), 7.27–7.25 (m, 1H), 6.75–6.73 (m, 1H), 4.09 (s, 3H), 3.71 (m, 1H), 3.37 (m, 2H), 2.81–2.75 (m, 2H), 2.25–2.21 (t, *J* = 7.6 Hz, 2H), 2.18–2.05 (m, 2H), 1.98–1.1.83 (m, 2H), 1.47–1.43 (m, 2H), 0.86 (t, *J* = 7.2 Hz, 3H). MS (ESI): [MH]⁺ = 424.3. Anal. (C₂₀H₂₅N₉O₂) C, H, N.

***N*-(1-Allylpiperidin-4-yl)-*N'*-[2-(2-furyl)-8-methyl-8H-pyrazolo[4,3-*e*]-[1,2,4]triazolo[1,5-*c*]pyrimidin-5-yl]urea (8).** White solid; 45% yield; mp 179 °C (dec); ¹H NMR (DMSO-*d*₆) δ 9.11 (bs, 1H), 8.77–8.72 (m, 2H), 7.98–7.97 (m, 1H), 7.30–7.28 (m, 1H), 6.76–6.74 (m, 1H), 5.95–5.76 (m, 1H), 5.23–5.16 (m, 2H), 4.12 (s, 3H), 3.79–3.71 (m, 1H), 2.99 (d, *J* = 5.8 Hz, 2H), 2.73 (m, 2H), 2.14–2.08 (m, 2H), 1.97–1.91 (m, 2H), 1.62–1.43 (m, 2H). MS (ESI): [MH]⁺ = 422.2. Anal. (C₂₀H₂₃N₉O₂) C, H, N.

***N*-[2-(2-Furyl)-8-methyl-8H-pyrazolo[4,3-*e*]-[1,2,4]triazolo[1,5-*c*]pyrimidin-5-yl]-*N'*-(1-prop-2-yn-1-ylpiperidin-4-yl)urea (9).** White solid; 38% yield; mp 212 °C (dec); ¹H NMR (DMSO-*d*₆) δ 9.11 (bs, 1H), 8.75 (s, 1H), 8.67 (bd, *J* = 7.6 Hz, 1H), 7.98–7.97 (m, 1H), 7.30–7.28 (m, 1H), 6.76–6.74 (m, 1H), 4.11 (s, 3H), 3.74–3.55 (m, 1H), 3.28 (s, 2H), 3.18 (s, 1H), 2.78–2.72 (m, 2H), 2.37–2.32 (m, 2H), 2.04–1.94 (m, 2H), 1.55–1.51 (m, 2H). MS (ESI): [MH]⁺ = 420.2. Anal. (C₂₀H₂₁N₉O₂) C, H, N.

***N*-(1-(Cyclohexylmethyl)piperidin-4-yl)-*N'*-[2-(2-furyl)-8-methyl-8H-pyrazolo[4,3-*e*]-[1,2,4]triazolo[1,5-*c*]pyrimidin-5-yl]urea (10).** White solid; 34% yield; mp 218 °C; ¹H NMR (DMSO-*d*₆) δ 8.97 (bs, 1H), 8.74 (m, 2H), 7.98 (m, 1H), 7.29 (m, 1H), 6.77 (m, 1H), 4.12 (s, 3H), 3.81 (m, 1H), 2.64 (m, 3H), 2.14–2.06 (m, 4H), 1.85 (m, 2H), 1.75–1.38 (m, 6H), 1.21–1.07 (m, 4H), 0.80 (m, 2H). MS (ESI): [MH]⁺ = 477.9. Anal. (C₂₄H₃₁N₉O₂) C, H, N.

***N*-(1-Benzylpiperidin-4-yl)-*N'*-[2-(2-furyl)-8-methyl-8H-pyrazolo[4,3-*e*]-[1,2,4]triazolo[1,5-*c*]pyrimidin-5-yl]urea (11).** White solid; 40% yield; mp 167 °C; ¹H NMR (DMSO-*d*₆) δ 8.99 (bs, 1H), 8.79 (m, 2H), 7.98 (m, 1H), 7.53–7.23 (m, 6H), 6.75 (m, 1H), 4.12 (s, 3H), 3.81 (m, 1H), 3.32 (s, 2H), 2.74 (m, 2H), 1.98–1.24 (m, 6H). MS (ESI): [MH]⁺ = 472.21. Anal. (C₂₄H₂₅N₉O₂) C, H, N.

***N*-(1-(4-Fluorobenzyl)piperidin-4-yl)-*N'*-[2-(2-furyl)-8-methyl-8H-pyrazolo[4,3-*e*]-[1,2,4]triazolo[1,5-*c*]pyrimidin-5-yl]urea (12).** White solid; 42% yield; mp 188 °C; ¹H NMR (DMSO-*d*₆) δ 9.12 (bs, 1H), 8.76 (bm, 2H), 7.97 (m, 1H), 7.37–7.14 (m, 5H), 6.76–6.74 (m, 1H), 4.12 (s, 3H), 3.71 (m, 1H), 3.48 (s, 2H), 2.73 (m, 2H), 2.12–1.83 (m, 4H), 1.59 (m, 2H). MS (ESI): [MH]⁺ = 490.2. Anal. (C₂₄H₂₄FN₉O₂) C, H, N.

***N*-(1-(4-Chlorobenzyl)piperidin-4-yl)-*N'*-[2-(2-furyl)-8-methyl-8H-pyrazolo[4,3-*e*]-[1,2,4]triazolo[1,5-*c*]pyrimidin-5-yl]urea (13).** White solid; 35% yield; mp 183 °C; ¹H NMR (DMSO-*d*₆) δ 9.07 (bs, 1H), 8.79–8.75 (bm, 2H), 7.97 (m, 1H), 7.37–7.28 (m, 5H), 6.76–6.74 (m, 1H), 4.12 (s, 3H), 3.78 (m, 1H), 3.49 (s, 2H), 2.72 (m, 2H), 2.20 (m, 2H), 1.95 (m, 2H), 1.56 (m, 2H). MS (ESI): [MH]⁺ = 506.0. Anal. (C₂₄H₂₄ClN₉O₂) C, H, N.

***N*-[2-(2-Furyl)-8-methyl-8H-pyrazolo[4,3-*e*]-[1,2,4]triazolo[1,5-*c*]pyrimidin-5-yl]-*N'*-[1-(4-methylbenzyl)piperidin-4-yl]urea (14).** White solid; 30% yield; mp 213 °C; ¹H NMR (DMSO-*d*₆) δ 9.08 (bs, 1H), 8.76–8.73 (bm, 2H), 7.97 (m, 1H), 7.29–7.11 (m, 5H), 6.76–6.74 (m, 1H), 4.12 (s, 3H), 3.76 (m, 1H), 3.44 (s, 2H),

2.68 (m, 2H), 2.28–2.11 (m, 5H), 1.98–1.89 (m, 2H), 1.54–1.49 (m, 2H). MS (ESI): $[MH]^+$ = 486.2. Anal. ($C_{23}H_{27}N_9O_2$) C, H, N.

N-[2-(2-Furyl)-8-methyl-8H-pyrazolo[4,3-e][1,2,4]triazolo[1,5-c]pyrimidin-5-yl]-N'-[1-(4-methoxybenzyl)piperidin-4-yl]urea (15). White solid; 33% yield; mp 217 °C; 1H NMR (DMSO- d_6) δ 9.08 (bs, 1H), 8.75 (m, 2H), 7.97 (m, 1H), 7.28 (m, 1H), 7.23 (dd, J = 8.6 Hz, 2H), 6.88 (d, J = 8.6 Hz, 2H), 6.75 (m, 1H), 4.12 (s, 3H), 3.73 (m, 4H), 3.42 (s, 2H), 2.71 (m, 2H), 2.21–2.12 (m, 2H), 1.95–1.90 (m, 2H), 1.58–1.49 (m, 2H). MS (ESI): $[MH]^+$ = 502.1. Anal. ($C_{23}H_{27}N_9O_3$) C, H, N.

N-[1-(4-Cyanobenzyl)piperidin-4-yl]-N'-[2-(2-furyl)-8-methyl-8H-pyrazolo[4,3-e][1,2,4]triazolo[1,5-c]pyrimidin-5-yl]urea (16). White solid; 30% yield; mp 239 °C; 1H NMR (DMSO- d_6) δ 8.74 (m, 3H), 7.97 (m, 1H), 7.80 (dd, J = 7.8 Hz, 2H), 7.55 (dd, J = 8 Hz, 2H), 7.28 (m, 1H), 6.77 (m, 1H), 4.12 (s, 3H), 3.79–3.60 (m, 3H), 2.69 (m, 2H), 2.18 (m, 2H), 1.95 (m, 2H), 1.59 (m, 2H). MS (ESI): $[MH]^+$ = 496.9. Anal. ($C_{25}H_{24}N_{10}O_2$) C, H, N.

N-[2-(2-Furyl)-8-methyl-8H-pyrazolo[4,3-e][1,2,4]triazolo[1,5-c]pyrimidin-5-yl]-N'-[1-(4-nitrobenzyl)piperidin-4-yl]urea (17). White solid; 48% yield; mp 228 °C; 1H NMR (DMSO- d_6) δ 9.18 (bs, 1H), 8.82–8.80 (bd, J = 7.2 Hz, 1H), 8.75 (s, 1H), 8.21 (dd, J = 8.8 Hz, 2H), 7.97 (m, 1H), 7.64 (dd, J = 8.8 Hz, 2H), 7.28 (m, 1H), 6.75 (m, 1H), 4.12 (s, 3H), 3.66 (m, 3H), 2.77–2.71 (m, 2H), 2.26 (m, 2H), 1.93 (m, 2H), 1.59 (m, 2H). MS (ESI): $[MH]^+$ = 516.9. Anal. ($C_{24}H_{24}N_{10}O_4$) C, H, N.

N-[2-(2-Furyl)-8-methyl-8H-pyrazolo[4,3-e][1,2,4]triazolo[1,5-c]pyrimidin-5-yl]-N'-[1-(pyridin-3-ylmethyl)piperidin-4-yl]urea (18). White solid; 29% yield; mp 226 °C; 1H NMR (DMSO- d_6) δ 9.13 (bs, 1H), 8.76–8.74 (bm, 2H), 8.52–8.45 (m, 2H), 7.98–7.97 (m, 1H), 7.77–7.71 (m, 1H), 7.39–7.33 (m, 1H), 7.30–7.28 (m, 1H), 6.76–6.74 (m, 1H), 4.12 (s, 3H), 3.68 (m, 1H), 3.54 (s, 2H), 2.76–2.70 (m, 2H), 2.27–2.17 (m, 2H), 1.99–1.90 (m, 2H), 1.61–1.51 (m, 2H). MS (ESI): $[MH]^+$ = 473.4. Anal. ($C_{23}H_{24}N_{10}O_2$) C, H, N.

N-[2-(2-Furyl)-8-methyl-8H-pyrazolo[4,3-e][1,2,4]triazolo[1,5-c]pyrimidin-5-yl]-N'-[1-(pyridin-4-ylmethyl)piperidin-4-yl]urea (19). White solid; 43% yield; mp 247 °C (dec); 1H NMR (DMSO- d_6) δ 9.08 (bs, 1H), 8.80–8.76 (bm, 2H), 8.51 (dd, J = 6.2 Hz, 2H), 7.98 (m, 1H), 7.35 (dd, J = 5.8 Hz, 2H), 7.29 (m, 1H), 6.75 (m, 1H), 4.12 (s, 3H), 3.69 (m, 1H), 3.55 (s, 2H), 2.76–2.70 (m, 2H), 2.29–2.19 (m, 2H), 1.99–1.93 (m, 2H), 1.64–1.54 (m, 2H). MS (ESI): $[MH]^+$ = 473.2. Anal. ($C_{23}H_{24}N_{10}O_2$) C, H, N.

Ethyl 4-[[[2-(2-Furyl)-8-methyl-8H-pyrazolo[4,3-e][1,2,4]triazolo[1,5-c]pyrimidin-5-yl]amino]carbonyl]amino]piperidin-1-yl]acetate (20). White solid; 50% yield; mp 207 °C; 1H NMR (DMSO- d_6) δ 9.11 (bs, 1H), 8.76 (bm, 2H), 7.98–7.97 (m, 1H), 7.30–7.28 (m, 1H), 6.76–6.74 (m, 1H), 4.15–4.04 (m, 5H), 3.69 (m, 1H), 3.24 (s, 2H), 2.75 (m, 2H), 2.40 (m, 2H), 1.98–1.82 (m, 2H), 1.61–1.42 (m, 2H), 1.20 (t, J = 7.2 Hz, 3H). MS (ESI): $[MH]^+$ = 468.2. Anal. ($C_{21}H_{25}N_9O_2$) C, H, N.

General Procedure for the Preparation of N-Substituted 4-[[[2-(2-Furyl)-8-methyl-8H-pyrazolo[4,3-e][1,2,4]triazolo[1,5-c]pyrimidin-5-yl]amino]carbonyl]amino]piperidine-1-carboxamide Derivatives 21–34. The chlorocarbonyl derivative 4 (90 mg, 0.2 mmol) was suspended in 1,4-dioxane (3 mL) and cooled to 0 °C. TEA (0.018 g, 0.18 mmol) and the appropriate amine (0.3 mmol) were then added, and the mixture was stirred for 1 h at 0 °C and for an additional 3 h at room temperature. The solvent was removed under reduce pressure, and the residue was purified by column chromatography, eluting with EtOAc (21–31), or via HPLC (33, 34).

N-Ethyl-4-[[[2-(2-furyl)-8-methyl-8H-pyrazolo[4,3-e][1,2,4]triazolo[1,5-c]pyrimidin-5-yl]amino]carbonyl]amino]piperidine-1-carboxamide (21). White solid; 30% yield; mp 192 °C; 1H NMR (DMSO- d_6) δ 9.14 (bs, 1H), 8.76 (bm, 2H), 7.98–7.97 (m, 1H), 7.29–7.28 (m, 1H), 6.76–6.75 (m, 1H), 6.52 (bm, 1H), 4.11 (s, 3H), 3.92–3.83 (m, 3H), 3.07–3.01 (m, 4H), 1.91 (m, 2H), 1.43 (m, 2H), 1.02 (t, J = 7.2 Hz, 3H). MS (ESI): $[MH]^+$ = 453.3. Anal. ($C_{20}H_{24}N_{10}O_3$) C, H, N.

4-[[[2-(2-Furyl)-8-methyl-8H-pyrazolo[4,3-e][1,2,4]triazolo[1,5-c]pyrimidin-5-yl]amino]carbonyl]amino]-N-isopropylpiperidine-1-carboxamide (22). White solid; 30% yield; mp 224 °C; 1H NMR (DMSO- d_6) δ 9.19 (bs, 1H), 8.74 (bm, 2H), 7.97 (m, 1H), 7.28 (m, 1H), 6.77–6.74 (m, 1H), 6.20 (bd, J = 7.8 Hz, 1H), 4.11 (s,

3H), 3.78–3.75 (m, 4H), 3.07 (m, 2H), 1.84 (m, 2H), 1.40 (m, 2H), 1.06 (d, J = 6.6 Hz, 6H). MS (ESI): $[MH]^+$ = 467.0. Anal. ($C_{21}H_{26}N_{10}O_3$) C, H, N.

N-Cyclopentyl-4-[[[2-(2-furyl)-8-methyl-8H-pyrazolo[4,3-e][1,2,4]triazolo[1,5-c]pyrimidin-5-yl]amino]carbonyl]amino]piperidine-1-carboxamide (23). White solid; 50% yield; mp 205 °C; 1H NMR (DMSO- d_6) δ 9.20 (bs, 1H), 8.79 (bd, J = 7.6 Hz, 1H), 8.73 (s, 1H), 7.97 (m, 1H), 7.28 (m, 1H), 6.76–6.73 (m, 1H), 6.27 (bd, J = 7 Hz, 1H), 4.10 (s, 3H), 3.93–3.74 (m, 4H), 3.03 (m, 2H), 1.90–1.35 (m, 12H). MS (ESI): $[MH]^+$ = 493.3. Anal. ($C_{23}H_{28}N_{10}O_3$) C, H, N.

N-Cyclohexyl-4-[[[2-(2-furyl)-8-methyl-8H-pyrazolo[4,3-e][1,2,4]triazolo[1,5-c]pyrimidin-5-yl]amino]carbonyl]amino]piperidine-1-carboxamide (24). White solid; 41% yield; mp 210 °C; 1H NMR (DMSO- d_6) δ 9.13 (bs, 1H), 8.75 (bm, 2H), 7.97 (m, 1H), 7.28 (m, 1H), 6.76 (m, 1H), 6.20 (bd, J = 7.6 Hz, 1H), 4.11 (s, 3H), 3.80–3.74 (m, 3H), 3.40 (m, 1H), 3.00 (m, 2H), 1.95–1.12 (m, 14 H). MS (ESI): $[MH]^+$ = 507.2. Anal. ($C_{24}H_{30}N_{10}O_3$) C, H, N.

N-Cycloheptyl-4-[[[2-(2-furyl)-8-methyl-8H-pyrazolo[4,3-e][1,2,4]triazolo[1,5-c]pyrimidin-5-yl]amino]carbonyl]amino]piperidine-1-carboxamide (25). White solid; 38% yield; mp 165 °C; 1H NMR (DMSO- d_6) δ 9.21 (bs, 1H), 8.76 (bm, 2H), 7.97 (m, 1H), 7.28 (m, 1H), 6.76–6.74 (m, 1H), 6.23 (d, J = 7.8 Hz, 1H), 4.11 (s, 3H), 3.77 (m, 4H), 3.05–2.94 (m, 2H), 1.90–1.75 (m, 16H). MS (ESI): $[MH]^+$ = 521.1. Anal. ($C_{25}H_{32}N_{10}O_3$) C, H, N.

N-Benzyl-4-[[[2-(2-furyl)-8-methyl-8H-pyrazolo[4,3-e][1,2,4]triazolo[1,5-c]pyrimidin-5-yl]amino]carbonyl]amino]piperidine-1-carboxamide (26). White solid; 39% yield; mp 227 °C; 1H NMR (DMSO- d_6) δ 9.13 (bs, 1H), 8.79 (bd, J = 7.6 Hz, 1H), 8.75 (s, 1H), 7.98–7.97 (m, 1H), 7.34–7.21 (m, 6H), 7.15 (m, 1H), 6.76–6.74 (m, 1H), 4.26 (d, J = 5.6 Hz, 2H), 4.12 (s, 3H), 3.89–3.81 (m, 3H), 3.10–3.04 (m, 2H), 1.93–1.89 (m, 2H), 1.45–1.38 (m, 2H). MS (ESI): $[MH]^+$ = 515.3. Anal. ($C_{25}H_{26}N_{10}O_3$) C, H, N.

4-[[[2-(2-Furyl)-8-methyl-8H-pyrazolo[4,3-e][1,2,4]triazolo[1,5-c]pyrimidin-5-yl]amino]carbonyl]amino]-N-(2-phenylethyl)piperidine-1-carboxamide (27). White solid; 63% yield; mp 216 °C; 1H NMR (DMSO- d_6) δ 9.17 (bs, 1H), 8.75 (bm, 2H), 7.97 (m, 1H), 7.31–7.18 (m, 6H), 6.75 (m, 1H), 6.72 (bt, J = 7 Hz, 1H), 4.11 (s, 3H), 3.80 (m, 3H), 3.24 (m, 2H), 3.05 (m, 2H), 2.73 (m, 2H), 1.82 (m, 2H), 1.40 (m, 2H). MS (ESI): $[MH]^+$ = 529.3. Anal. ($C_{26}H_{28}N_{10}O_3$) C, H, N.

4-[[[2-(2-Furyl)-8-methyl-8H-pyrazolo[4,3-e][1,2,4]triazolo[1,5-c]pyrimidin-5-yl]amino]carbonyl]amino]-N-(3-phenylpropyl)piperidine-1-carboxamide (28). White solid; 39% yield; mp 218 °C; 1H NMR (DMSO- d_6) δ 9.13 (bs, 1H), 8.75 (bm, 2H), 7.97 (m, 1H), 7.29–7.16 (m, 6H), 6.76–6.74 (m, 1H), 6.55 (bt, J = 7 Hz, 1H), 4.10 (s, 3H), 3.81–3.74 (m, 3H), 3.07–3.02 (m, 4H), 2.61–2.53 (m, 2H), 1.95–1.72 (m, 4H), 1.41 (m, 2H). MS (ESI): $[MH]^+$ = 543.3. Anal. ($C_{27}H_{30}N_{10}O_3$) C, H, N.

N-(4-Fluorobenzyl)-4-[[[2-(2-furyl)-8-methyl-8H-pyrazolo[4,3-e][1,2,4]triazolo[1,5-c]pyrimidin-5-yl]amino]carbonyl]amino]piperidine-1-carboxamide (29). White solid; 30% yield; mp 217 °C; 1H NMR (DMSO- d_6) δ 9.19 (bs, 1H), 8.78 (bd, J = 7.6 Hz, 1H), 8.75 (s, 1H), 7.97 (m, 1H), 7.34–7.26 (m, 3H), 7.19–7.14 (m, 3H), 6.75 (m, 1H), 4.23 (d, J = 5.6 Hz, 2H), 4.12 (s, 3H), 3.86–3.79 (m, 3H), 3.06 (m, 2H), 1.89 (m, 2H), 1.40 (m, 2H). MS (ESI): $[MH]^+$ = 533.2. Anal. ($C_{25}H_{25}FN_{10}O_3$) C, H, N.

N-(4-Chlorobenzyl)-4-[[[2-(2-furyl)-8-methyl-8H-pyrazolo[4,3-e][1,2,4]triazolo[1,5-c]pyrimidin-5-yl]amino]carbonyl]amino]piperidine-1-carboxamide (30). White solid; 36% yield; mp 186 °C (dec); 1H NMR (DMSO- d_6) δ 8.80–8.77 (bm, 3H), 7.98 (m, 1H), 7.50–7.49 (m, 1H), 7.38 (d, J = 8.4 Hz, 2H), 7.28 (dd, J = 8.4 Hz, 2H), 7.20 (bm, 1H), 6.76–6.75 (m, 1H), 4.23 (d, J = 5.6 Hz, 2H), 4.12 (s, 3H), 3.84–3.80 (m, 3H), 3.06 (m, 2H), 1.92–1.89 (m, 2H), 1.42–1.40 (m, 2H). MS (ESI): $[MH]^+$ = 549.5. Anal. ($C_{25}H_{25}ClN_{10}O_3$) C, H, N.

4-[[[2-(2-Furyl)-8-methyl-8H-pyrazolo[4,3-e][1,2,4]triazolo[1,5-c]pyrimidin-5-yl]amino]carbonyl]amino]-N-(4-methylbenzyl)piperidine-1-carboxamide (31). White solid; 45% yield; mp 232 °C; 1H NMR (DMSO- d_6) δ 9.12 (bs, 1H), 8.80–8.75 (bm, 2H), 7.97 (m, 1H), 7.28 (m, 1H), 7.18–7.07 (m, 5H), 6.75 (m, 1H), 4.21 (d, J = 5.6 Hz, 2H), 4.12 (s, 3H), 3.86–3.79 (m, 3H), 3.11–

3.00 (m, 2H), 2.27 (s, 3H), 1.93–1.88 (m, 2H), 1.43–1.36 (m, 2H). MS (ESI): $[MH]^+ = 529.0$. Anal. ($C_{26}H_{28}N_{10}O_3$) C, H, N.

4-[[[2-(2-Furyl)-8-methyl-8H-pyrazolo[4,3-e][1,2,4]triazolo[1,5-c]pyrimidin-5-yl]amino]carbonyl]amino]-N-(4-methoxybenzyl)piperidine-1-carboxamide (32). White solid; 45% yield; mp 224 °C; 1H NMR (DMSO- d_6) δ 9.18 (bs, 1H), 8.81 (bd, $J = 7.8$ Hz, 1H), 8.73 (s, 1H), 7.96 (m, 1H), 7.27 (m, 1H), 7.19 (dd, $J = 8.8$ Hz, 2H), 7.04 (bt, $J = 5.6$ Hz, 1H), 6.87 (dd, $J = 8.8$ Hz, 2H), 6.76–6.73 (m, 1H), 4.18 (d, $J = 5.6$ Hz, 2H), 4.10 (s, 3H), 3.84 (m, 3H), 3.72 (s, 3H), 3.02 (m, 2H), 1.83 (m, 2H), 1.42 (m, 2H). MS (ESI): $[MH]^+ = 545.2$. Anal. ($C_{26}H_{28}N_{10}O_4$) C, H, N.

4-[[[2-(2-Furyl)-8-methyl-8H-pyrazolo[4,3-e][1,2,4]triazolo[1,5-c]pyrimidin-5-yl]amino]carbonyl]amino]-N-pyridin-4-ylpiperidine-1-carboxamide Trifluoroacetate (33). White solid; 41% yield; mp 157 °C; 1H NMR (DMSO- d_6) δ 10.2 (bs, 1H), 9.22 (bs, 1H), 8.77 (m, 2H), 8.56 (dd, $J = 7.2$ Hz, 2H), 7.98 (m, 1H), 7.91 (dd, $J = 7.4$ Hz, 2H), 7.30 (m, 1H), 6.77–6.75 (m, 1H), 4.11 (s, 3H), 4.02 (m, 3H), 3.39 (m, 2H), 2.17–2.03 (m, 2H), 1.66–1.43 (m, 2H). MS (ESI): $[MH]^+ = 502.4$. Anal. ($C_{25}H_{23}F_3N_{11}O_5$) C, H, N.

4-[[[2-(2-Furyl)-8-methyl-8H-pyrazolo[4,3-e][1,2,4]triazolo[1,5-c]pyrimidin-5-yl]amino]carbonyl]amino]-N-(4-methylpiperazin-1-yl)piperidine-1-carboxamide Trifluoroacetate (34). White solid; 44% yield; mp 101 °C; 1H NMR (DMSO- d_6) δ 9.79 (bs, 1H), 9.16 (bs, 1H), 8.77 (m, 2H), 7.98 (m, 1H), 7.30 (m, 1H), 6.77–6.74 (m, 1H), 4.11 (s, 3H), 3.81 (m, 3H), 3.71–3.43 (m, 6H), 3.08–3.02 (m, 4H), 2.82 (s, 3H), 2.01–1.91 (m, 2H), 1.61–1.41 (m, 2H). MS (ESI): $[MH]^+ = 507.8$. Anal. ($C_{25}H_{23}F_3N_{11}O_5$) C, H, N.

Biology. Evaluation of Affinity (K_i) and Potency (IC_{50}) of the Novel Adenosine Compounds. CHO (Chinese Hamster Ovary) Membranes Preparation. The human A_{1A} , A_{2A} , A_{2B} , and A_3 adenosine receptors have been transfected in CHO cells according to the method previously described.³¹ The cells were grown adherently and maintained in Dulbecco's modified Eagle's medium with nutrient mixture F12 (DMEM/F12) without nucleosides, containing 10% fetal calf serum, penicillin (100 U/mL), streptomycin (100 μ g/mL), L-glutamine (2 mM), and Geneticin (G418, 0.2 mg/mL) at 37 °C in 5% CO_2 , 95% air. For membrane preparation the culture medium was removed and the cells were washed with PBS and scraped off T75 flasks in ice-cold hypotonic buffer (5 mM Tris-HCl, 2 mM EDTA, pH 7.4). The cell suspension was homogenized with a Polytron, and the homogenate was centrifuged for 10 min at 1000g. The supernatant was then centrifuged for 30 min at 100000g. The membrane pellet was suspended in (a) 50 mM Tris-HCl buffer, pH 7.4, for A_1 ARs; (b) 50 mM Tris-HCl, 10 mM $MgCl_2$ buffer, pH 7.4, for A_{2A} ARs; (c) 50 mM Tris-HCl, 10 mM $MgCl_2$, 1 mM EDTA buffer, pH 7.4, for A_3 ARs. The cell suspension was incubated with 2 IU/mL of adenosine deaminase for 30 min at 37 °C. The membrane preparation was used to perform binding experiments.

Human Cloned A_1 , A_{2A} , and A_3 Adenosine Receptor Binding Assay. All synthesized compounds have been tested for their affinity to human A_1 , A_{2A} , and A_3 ARs. Displacement binding experiments of [3H]DPCPX (1 nM) to hA_1 CHO membranes (50 μ g of protein/assay) and at least six to eight different concentrations of examined antagonists were performed for 120 min at 25 °C. Nonspecific binding was determined in the presence of 1 μ M DPCPX, and this was always $\leq 10\%$ of the total binding.³² Inhibition binding experiments of [3H]ZM241385 (2 nM) to hA_{2A} CHO membranes (50 μ g of protein/assay) and at least six to eight different concentrations of the studied compounds were performed for 60 min at 4 °C. Nonspecific binding was determined in the presence of 1 μ M ZM241385 and was about 20% of total binding.³³ Competition binding experiments of [3H]MRE-3008-F20 (1 nM) to hA_3 CHO membranes (50 μ g of protein/assay) and at least six to eight different concentrations of examined ligands were performed for 120 min at 4 °C. Nonspecific binding was defined as binding in the presence of 1 μ M MRE-3008-F20 and was about 25% of total binding.³⁴ Bound and free radioactivity was separated by filtering the assay mixture through Whatman GF/B glass fiber filters which were washed three times with ice-cold buffer. The filter bound radioactivity was counted by using a Packard Tri Carb 2810 TR scintillation counter (Perkin-Elmer).

Measurement of Cyclic AMP Levels in CHO Cells Transfected with Human A_{2B} and A_3 Adenosine Receptors. CHO cells transfected with human A_{2B} AR or A_3 AR were washed with phosphate buffered saline, diluted trypsin and centrifuged for 10 min at 200g. The pellet containing CHO cells (1×10^6 cells/assay) was suspended in 0.5 mL of incubation mixture (mM): NaCl 15, KCl 0.27, NaH_2PO_4 0.037, $MgSO_4$ 0.1, $CaCl_2$ 0.1, Hepes 0.01, $MgCl_2$ 1, glucose 0.5, pH 7.4 at 37 °C, 2 IU/mL adenosine deaminase, and 4-(3-butoxy-4-methoxybenzyl)-2-imidazolidinone (Ro 20-1724) as phosphodiesterase inhibitor. The mixture was preincubated for 10 min in a shaking bath at 37 °C. The potency of the antagonists versus hA_{2B} ARs was determined by antagonism of NECA (100 nM) induced stimulation of cyclic AMP levels.³⁵ In addition, the potency of the antagonists to hA_3 ARs was determined in the presence of 1 μ M forskolin by antagonism of Cl-IB-MECA (100 nM) induced inhibition of cyclic AMP levels.³⁴ The reaction was terminated by the addition of cold 6% trichloroacetic acid (TCA). The TCA suspension was centrifuged at 2000g for 10 min at 4 °C, and the supernatant was extracted four times with water saturated diethyl ether. The final aqueous solution was tested for cyclic AMP levels by a competition protein binding assay. Samples of cyclic AMP standard (0–10 pmol) were added to each test tube containing the incubation buffer (0.1 M Trizma base, 8.0 mM aminophylline, 6.0 mM 2 mercaptoethanol, pH 7.4) and [3H] cyclic AMP in a total volume of 0.5 mL. The binding protein was added to the samples and incubated at 4 °C for 150 min. The samples, after the addition of charcoal, were centrifuged at 2000g for 10 min. The clear supernatant was counted by using a Packard Tri Carb 2810 TR scintillation counter (Perkin-Elmer).

Data Analysis. The protein concentration was determined according to a Bio-Rad method³⁶ with bovine albumin as a standard reference. Inhibitory binding constants, K_i , were calculated from the IC_{50} values according to the Cheng and Prusoff equation³⁷ $K_i = IC_{50}/(1 + [C^*]/K_D^*)$, where $[C^*]$ is the concentration of the radioligand and K_D^* its dissociation constant. A weighted nonlinear least-squares curve fitting program LIGAND³⁸ was also used for computer analysis of inhibition experiments. Potency values (IC_{50}) obtained in cyclic AMP assays were calculated by nonlinear regression analysis using the equation for a sigmoid concentration–response curve (GraphPad Prism, San Diego, CA, U.S.). All experimental data are expressed as geometric mean with 95% confidence limits in parentheses of three or four independent experiments performed in duplicate.

Molecular Modeling. Receptor Docking. Prior to docking calculations, the Epik software was used to calculate the most relevant ionization and tautomeric state of compounds **10**.³⁹ Then the Glide program of the Schrodinger package⁴⁰ was used to dock **10** to the hA_3 AR structure. The receptor grid generation was performed for the box with a center in the putative binding site. The size of the box was determined automatically. The extra precision mode (XP) of Glide was used for docking. The ligand scaling factor was set to 1.0. The geometry of the ligand binding site of the complex between **10** and the receptor was then optimized. The binding site was defined as **10** and all amino acid residues located within 8 Å from the ligand. All the receptor residues located within 2 Å from the binding site were used as a shell. The following parameters of energy minimization were used: OPLS2005 force field was used. Water was used as an implicit solvent, and a maximum of 5000 iterations of the Polak–Ribier conjugate gradient minimization method was used with a convergence threshold of 0.01 kJ mol $^{-1}$ Å $^{-1}$. All complex pictures were rendered employing the UCSF Chimera software.⁴¹

■ ASSOCIATED CONTENT

Supporting Information

Additional table reporting the predicted PK parameters. This material is available free of charge via the Internet at <http://pubs.acs.org>.

AUTHOR INFORMATION

Corresponding Author

*Phone: +39-0532-455921. Fax: +39-0532-455921. E-mail: baraldi@unife.it.

Present Address

#Alta Vetta Pharmaceutical Consulting, LLC, 3 Skipwith Court, Durham, North Carolina 27707.

Notes

The authors declare no competing financial interest.

ACKNOWLEDGMENTS

We thank King Pharmaceuticals, Inc., Research and Development, NC, for financial support. We also thank Prof. Karl-Norbert Klotz for cDNA encoding the human adenosine receptors. The authors thank Dr. Erika Marzola for technical assistance.

ABBREVIATIONS USED

AR, adenosine receptor; CHO, Chinese hamster ovary; Cl-IB-MECA, 2-chloro-N⁶-(3-iodobenzyl)adenosine-5'-N-methylcarboxamide; DMEM, Dulbecco's modified Eagle's medium; EtOAc, ethyl acetate; IP₃, inositol 1,4,5-trisphosphate; NECA, 5'-(N-ethylcarboxamido)adenosine; PTP, pyrazolo[4,3-*e*]-[1,2,4]triazolo[1,5-*c*]pyrimidine; TEA, triethylamine

REFERENCES

- (1) Fredholm, B. B.; Arslan, G.; Halldner, L.; Kull, B.; Shulte, G.; Wasserman, W. Structure and function of adenosine receptors and their genes. *Naunyn-Schmiedeberg's Arch. Pharmacol.* **2000**, *362*, 364–374.
- (2) Murphree, L. J.; Linden, J. Adenosine receptors. *Encycl. Biol. Chem.* **2004**, *1*, 34–39.
- (3) Jacobson, K. A.; Knutsen, L. J. S. P1 and P2 purine and pyrimidine receptor ligands. *Handb. Exp. Pharmacol.* **2001**, *151*, 129–175.
- (4) Fredholm, B. B.; AP, I. J.; Jacobson, K. A.; Linden, J.; Muller, C. E. International Union of Basic and Clinical Pharmacology. LXXXI. Nomenclature and classification of adenosine receptors: an update. *Pharmacol. Rev.* **2011**, *63*, 1–34.
- (5) Van Schaick, E. A.; Jacobson, K. A.; Kim, H. O.; IJzerman, A. P.; Danhof, M. Hemodynamic effects and histamine release elicited by the selective adenosine A₃ receptor agonist Cl-IB-MECA in conscious rats. *Eur. J. Pharmacol.* **1996**, *308*, 311–314.
- (6) Hannon, J. P.; Pfannkuche, H. J.; Fozard, J. R. A role for mast cells in adenosine A₃ receptor-mediated hypotension in the rat. *Br. J. Pharmacol.* **1995**, *115*, 945–952.
- (7) Baraldi, P. G.; Tabrizi, M. A.; Gessi, S.; Borea, P. A. Adenosine receptor antagonists: translating medicinal chemistry and pharmacology into clinical utility. *Chem. Rev.* **2008**, *108*, 238–263.
- (8) Borea, P.; Gessi, S.; Bar-Yehuda, S.; Fishman, P. A₃ adenosine receptor: pharmacology and role in disease. *Handb. Exp. Pharmacol.* **2009**, *193*, 297–327.
- (9) Wang, Z.; Do, C. W.; Avila, M. Y.; Peterson-Yantorno, K.; Stone, R. A.; Gao, Z. G.; Joshi, B.; Besada, P.; Jeong, L. S.; Jacobson, K. A.; Civan, M. M. Nucleoside-derived antagonists to A₃ adenosine receptors lower mouse intraocular pressure and act across species. *Exp. Eye Res.* **2010**, *90*, 146–154.
- (10) Yang, H.; Avila, M. Y.; Peterson-Yantorno, K.; Coca-Prados, M.; Stone, R. A.; Jacobson, K. A.; Civan, M. M. The cross-species A₃ adenosine receptor antagonist MRS 1292 inhibits adenosine-triggered human nonpigmented ciliary epithelial cell fluid release and reduces mouse intraocular pressure. *Curr. Eye Res.* **2005**, *30*, 747–754.
- (11) Gessi, S.; Cattabriga, E.; Avitabile, A.; Gafa', R.; Lanza, G.; Cavazzini, L.; Bianchi, N.; Gambari, R.; Feo, C.; Liboni, A.; Gullini, S.; Leung, E.; Mac-Lennan, S.; Borea, P. A. Elevated expression of A₃

adenosine receptors in human colorectal cancer is reflected in peripheral blood cells. *Clin. Cancer Res.* **2004**, *10*, 5895–5901.

- (12) Baraldi, P. G.; Cacciari, B.; Romagnoli, R.; Spalluto, G.; Monopoli, A.; Ongini, E.; Varani, K.; Borea, P. A. 7-Substituted 5-amino-2-(2-furyl)pyrazolo[4,3-*e*]-1,2,4-triazolo[1,5-*c*]pyrimidines as A_{2A} adenosine receptor antagonists: a study on the importance of modifications at the side chain on the activity and solubility. *J. Med. Chem.* **2002**, *45*, 115–126.

- (13) Baraldi, P. G.; Tabrizi, M. A.; Romagnoli, R.; El-Kashef, H.; Preti, D.; Bovero, A.; Fruttarolo, F.; Gordaliza, M.; Borea, P. A. Pyrazolo[4,3-*e*][1,2,4]triazolo[1,5-*c*]pyrimidine template: organic and medicinal chemistry approach. *Curr. Org. Chem.* **2006**, *10*, 259–275.

- (14) Baraldi, P. G.; Fruttarolo, F.; Tabrizi, M. A.; Preti, D.; Romagnoli, R.; El-Kashef, H.; Moorman, A.; Varani, K.; Gessi, S.; Merighi, S.; Borea, P. A. Design, synthesis, and biological evaluation of C⁹- and C²-substituted pyrazolo[4,3-*e*]-1,2,4-triazolo[1,5-*c*]pyrimidines as new A_{2A} and A₃ adenosine receptors antagonists. *J. Med. Chem.* **2003**, *46*, 1229–1241.

- (15) Maconi, A.; Pastorin, G.; Da Ros, T.; Spalluto, G.; Gao, Z. G.; Jacobson, K. A.; Baraldi, P. G.; Cacciari, B.; Varani, K.; Moro, S.; Borea, P. A. Synthesis, biological properties, and molecular modeling investigation of the first potent, selective, and water-soluble human A₃ adenosine receptor antagonist. *J. Med. Chem.* **2002**, *45*, 3579–3582.

- (16) Baraldi, P. G.; Saponaro, G.; Tabrizi, M. A.; Baraldi, S.; Romagnoli, R.; Moorman, A.; Varani, K.; Borea, P. A.; Preti, D. Pyrrolo- and pyrazolo-[3,4-*e*][1,2,4]triazolo[1,5-*c*]pyrimidines as adenosine receptor antagonists. *Bioorg. Med. Chem.* **2012**, *20*, 1046–1059.

- (17) Cheong, S. L.; Dolzhenko, A. V.; Paoletta, S.; Lee, E. P. R.; Kachler, S.; Federico, S.; Klotz, K. N.; Dolzhenko, A. V.; Spalluto, G.; Moro, S.; Pastorin, G. Does the combination of optimal substitutions at the C², N⁵- and N⁸-positions of the pyrazolo-triazolo-pyrimidine scaffold guarantee selective modulation of the human A₃ adenosine receptors? *Bioorg. Med. Chem.* **2011**, *19*, 6120–6134.

- (18) Cheong, S. L.; Dolzhenko, A.; Kachler, S.; Paoletta, S.; Federico, S.; Cacciari, B.; Dolzhenko, A.; Klotz, K. N.; Moro, S.; Spalluto, G.; Pastorin, G. The significance of 2-furyl ring substitution with a 2-(para-substituted) aryl group in a new series of pyrazolo-triazolo-pyrimidines as potent and highly selective hA₃ adenosine receptors antagonists: new insights into structure–affinity relationship and receptor–antagonist recognition. *J. Med. Chem.* **2010**, *53*, 3361–3375.

- (19) Baraldi, P. G.; Borea, P. A. New potent and selective human adenosine A₃ receptor antagonists. *Trends Pharmacol. Sci.* **2000**, *21*, 456–459.

- (20) Varani, K.; Merighi, S.; Gessi, S.; Klotz, K. N.; Leung, E.; Baraldi, P. G.; Cacciari, B.; Romagnoli, R.; Spalluto, G.; Borea, P. A. [³H]-MRE 3008-F20: a novel antagonist radioligand for the pharmacological and biochemical characterization of human A₃ adenosine receptors. *Mol. Pharmacol.* **2000**, *57*, 968–975.

- (21) Merighi, S.; Mirandola, P.; Varani, K.; Gessi, S.; Capitani, S.; Leung, E.; Baraldi, P. G.; Tabrizi, M. A.; Borea, P. A. Pyrazolotriazolopyrimidine derivatives sensitize melanoma cells to the chemotherapeutic drugs: Taxol and vindesine. *Biochem. Pharmacol.* **2003**, *66*, 739–748.

- (22) Baraldi, P. G.; Bovero, A.; Fruttarolo, F.; Romagnoli, R.; Tabrizi, M. A.; Preti, D.; Varani, K.; Borea, P. A.; Moorman, A. R. New strategies for the synthesis of A₃ adenosine receptor antagonists. *Bioorg. Med. Chem.* **2003**, *11*, 4161–4169.

- (23) Banwell, M. G.; Coster, M. J.; Harvey, M. J.; Moraes, J. Selective cleavage of N-benzyl-protected secondary amines by triphosgene. *J. Org. Chem.* **2003**, *68*, 613–616.

- (24) Jorand-Lebrun, C.; Valognes, D.; Halazy, S. Use of triphosgene for direct preparation of carbamoyl chlorides from tertiary benzylamines. *Synth. Commun.* **1998**, *28*, 1189–1195.

- (25) Westendorf, A. F.; Zerzankova, L.; Salassa, L.; Sadler, P. J.; Brabec, V.; Bednarski, P. J. Influence of pyridine versus piperidine ligands on the chemical, DNA binding and cytotoxic properties of light activated trans,trans,trans-[Pt(N₃)₂(OH)₂(NH₃)(L)]. *J. Inorg. Biochem.* **2011**, *105*, 652–662.

(26) Baraldi, P. G.; Preti, D.; Zaid, A. N.; Saponaro, G.; Tabrizi, M. A.; Baraldi, S.; Romagnoli, R.; Moorman, A. R.; Varani, K.; Cosconati, S.; Di Maro, S.; Marinelli, L.; Novellino, E.; Borea, P. A. New 2-heterocyclyl-imidazo[2,1-*i*]purin-5-one derivatives as potent and selective human A₃ adenosine receptor antagonists. *J. Med. Chem.* **2011**, *54*, 5205–5320.

(27) Jaakola, V. P.; Griffith, M. T.; Hanson, M. A.; Cherezov, V.; Chien, E. Y.; Lane, J. R.; Ijzerman, A. P.; Stevens, R. C. The 2.6 angstrom crystal structure of a human A_{2A} adenosine receptor bound to an antagonist. *Science* **2008**, *322*, 1211–1217.

(28) Lenzi, O.; Colotta, V.; Catarzi, D.; Varano, F.; Poli, D.; Filacchioni, G.; Varani, K.; Vincenzi, F.; Borea, P. A.; Paoletta, S.; Morizzo, E.; Moro, S. 2-Phenylpyrazolo[4,3-*d*]pyrimidin-7-one as a new scaffold to obtain potent and selective human A₃ adenosine receptor antagonists: new insights into the receptor–antagonist recognition. *J. Med. Chem.* **2009**, *52*, 7640–7652.

(29) Gao, Z.-G.; Chen, A.; Barak, D.; Kim, S.-K.; Muller, C. E.; Jacobson, K. A. Identification by site-directed mutagenesis of residues involved in ligand recognition and activation of the human A₃ adenosine receptor. *J. Biol. Chem.* **2002**, *277*, 19056–19063.

(30) Rydberg, P.; Gloriam, D. E.; Zaretski, J.; Breneman, C.; Olsen, L. SMARTCyp: a 2D method for prediction of cytochrome P450-mediated drug metabolism. *ACS Med. Chem. Lett.* **2010**, *1*, 96–100.

(31) Klotz, K. N.; Hessling, J.; Hegler, J.; Owman, C.; Kull, B.; Fredholm, B. B.; Lohse, M. J. Comparative pharmacology of human adenosine receptor subtypes—characterization of stably transfected receptors in CHO cells. *Naunyn-Schmiedeberg's Arch. Pharmacol.* **1998**, *357*, 1–9.

(32) Borea, P. A.; Dalpiaz, A.; Varani, K.; Gessi, S.; Gilli, G. Binding thermodynamics of adenosine A_{2A} receptor ligands. *Biochem. Pharmacol.* **1995**, *49*, 461–469.

(33) Borea, P. A.; Dalpiaz, A.; Varani, K.; Gessi, S.; Gilli, G. Binding thermodynamics at A₁ and A_{2A} adenosine receptors. *Life Sci.* **1996**, *59*, 1373–1388.

(34) Varani, K.; Merighi, S.; Gessi, S.; Klotz, K. N.; Leung, E.; Baraldi, P. G.; Cacciari, B.; Romagnoli, R.; Spalluto, P.; Borea, P. A. [³H]-MRE3008F20: a novel antagonist radioligand for the pharmacological and biochemical characterization of human A₃ adenosine receptors. *Mol. Pharmacol.* **2000**, *57*, 968–975.

(35) Varani, K.; Gessi, S.; Merighi, S.; Vincenzi, F.; Cattabriga, E.; Benini, A.; Klotz, K. N.; Baraldi, P. G.; Tabrizi, M. A.; Mac Lennan, S.; Leung, E.; Borea, P. A. Pharmacological characterization of novel adenosine ligands in recombinant and native human A_{2B} receptors. *Biochem. Pharmacol.* **2005**, *70*, 1601–1612.

(36) Bradford, M. M. A rapid and sensitive method for the quantification of microgram quantities of protein utilizing the principle of protein dye-binding. *Anal. Biochem.* **1976**, *72*, 248–254.

(37) Cheng, Y. C.; Prusoff, W. H. Relationships between the inhibition constant (K_i) and the concentration of inhibitor which causes 50 per cent inhibition (IC₅₀) of an enzymatic reaction. *Biochem. Pharmacol.* **1973**, *22*, 3099–3108.

(38) Munson, P. J.; Rodbard, D. Ligand: a versatile computerized approach for the characterization of ligand binding systems. *Anal. Biochem.* **1980**, *107*, 220–239.

(39) *Epik*, version 2.0; Schrödinger, LLC: New York, NY, 2009.

(40) *Glide*; Schrödinger, LLC: New York, NY, 2008.

(41) Pettersen, E. F.; Goddard, T. D.; Huang, C. C.; Couch, G. S.; Greenblatt, D. M.; Meng, E. C.; Ferrin, T. E. UCSF Chimera—a visualization system for exploratory research and analysis. *J. Comput. Chem.* **2004**, *25*, 1605–1612.

(42) Taliani, S.; Pugliesidd, I.; Barresi, E.; Simorini, F.; Salerno, S.; La Motta, C.; Marini, A. M.; Cosimelli, B.; Cosconati, S.; Di Maro, S.; Marinelli, L.; Daniele, S.; Trincavelli, M. L.; Greco, G.; Novellino, E.; Martini, C.; Da Settimo, F. 3-Aryl-[1,2,4]triazino[4,3-*a*]benzimidazol-4(10*H*)-one: a novel template for the design of highly selective A_{2B} adenosine receptor antagonists. *J. Med. Chem.* **2012**, *55*, 1490–1499.